Two birds with one stone: a novel potential antibiotic blocking IsdB-mediated heme extraction by *Staphylococcus aureus* with serendipitous hemoglobin left-shifting activity

Sarah Hijazi[1¶], Francesco Marchesani[2¶], Marialaura Marchetti[2¶], Valeria Buoli Comani[3], Paul Brear[4], Barbara Campanini[3], Luca Ronda[2,5], Serena Faggiano[3,5], Eleonora Gianquinto[6], Somayeh Asghar Pour Hassan Kiyadeh[6], Barbara Rolando[6], Francesca Spyrakis[6], Carlotta Compari[3], Loretta Lazzarato[6*], Omar De Bei[2*], Emanuela Frangipani[1*], Stefano Bettati[2,5]

[1] *Department of Biomolecular Sciences, University of Urbino Carlo Bo, Urbino, Italy*

[2] *Department of Medicine and Surgery, University of Parma, Parma, Italy*

[3] *Department of Food and Drug, University of Parma, Parma, Italy*

[4] *Department of Biochemistry, University of Cambridge, Cambridge, United Kingdom*

[5] *Institute of Biophysics, National Research Council (CNR), Pisa, Italy*

[6] *Department of Drug Science and Technology, University of Turin, Turin, Italy.*

¶ Contributed equally to the work

* Corresponding authors

E-mail: omar.debei@unipr.it

Abstract

Infections caused by *Staphylococcus aureus* are closely linked to its ability to secure essential nutrients, including iron, which is extracted from the heme of human hemoglobin (Hb) through the iron-regulated surface determinant (Isd) system. The compound 4-[[2-[[5-(1H-indol-3-yl)-1,3,4-oxadiazol-2-yl]sulfanyl]acetyl]amino]benzoate (C35) was recently identified as a new potential antimicrobial agent for its ability to bind Hb and hamper its interaction with the staphylococcal hemophore IsdB *in vitro*. Here, we show that C35 inhibits *S. aureus* growth by specifically targeting the hemophore-driven iron acquisition system. Our findings confirm both the potential of C35 as a first-in-class protein-protein interaction inhibitor with antimicrobial activity, and the effectiveness of targeting hemophores as a strategy to inhibit *S. aureus* growth. To gain information for drug discovery purposes, the X-ray structure of Hb in the presence of the compound was solved. Unexpectedly, we discovered that, rather than the predicted binding pose, the molecule binds to tetrameric Hb in a cleft between the alpha subunits, stabilizing an R2 relaxed Hb conformation. This triggered further investigation of the effect of C35 on Hb functional properties, which showed a pronounced left-shift activity on oxygen binding curve (i.e., it strongly increases the Hb oxygen affinity). These results highlight C35 as a promising dual-acting compound with both antimicrobial activity and the ability to modulate Hb function through non-covalent stabilization of a high-affinity state.

Author Summary

Staphylococcus aureus is a dangerous bacterium that can cause severe infections in humans. To grow and survive it needs iron, which it steals from our red blood cells by taking it from hemoglobin, the protein that carries oxygen in the blood. In this study, we focused on a small molecule, called C35, that blocks the interaction between hemoglobin and a key

bacterial protein involved in heme acquisition. We found that C35 strongly inhibits the growth of *S. aureus* when hemoglobin is the only available source of iron, showing a potential new method to starve the pathogen and consequently fight the infection. Surprisingly, we also found that C35 increases the affinity of hemoglobin for oxygen. This dual action makes C35 a unique molecule for future therapeutic development, with potential applications both as a new antimicrobial agent and in the treatment of diseases related to hemoglobin function.

Introduction

Staphylococcus aureus is a human commensal and opportunistic pathogen capable of causing severe infections. Its ability to develop resistance to antibiotics highlights the urgent need for new, effective antimicrobial agents [1]. *S. aureus* depends on iron for survival; in the human body, this metal is primarily associated with heme cofactor in hemoglobin (Hb). With the aim of gaining access to the hemic iron, during infection *S. aureus* induces red blood cell (RBC) hemolysis exploiting hemolysins, thus allowing access to free Hb [2]. Iron gain is mediated by the iron-regulated surface determinant (Isd) system, a nine-protein gear in charge of intercepting Hb, extracting heme and internalizing it [3]. During the first step, the cell wall-anchored hemophore IsdB interacts with circulating Hb [4] and extracts the heme [5], which is transferred to other proteins of the Isd system in order to complete the iron acquisition process [2]. IsdB is a multifaceted protein that plays a crucial role in *S. aureus* virulence by facilitating iron acquisition, promoting adherence to host tissues, and modulating the host immune response [6–9]. Due to its significant role in *S. aureus* pathogenesis, IsdB has been explored as a potential vaccine candidate. However, clinical trials have proven unsuccessful, underscoring the need for innovative antibacterial strategies to combat *S. aureus* infections [10]. One promising approach is the discovery of chemical entities able to counteract the IsdB:Hb complex formation [11]. With this purpose,

71 in a recent work we conducted a virtual screening campaign targeting the IsdB:Hb complex,
72 and *in vitro* binding tests led to the identification of 4-[[2-[[5-(1H-indol-3-yl)-1,3,4-oxadiazol-
73 2-yl]sulfanyl]acetyl]amino]benzoate (C35) as the most potent molecule, with a K_D for Hb of
74 0.57 ± 0.06 μM [12]. In this work, we performed microbiological tests that proved the C35
75 effectiveness in inhibiting *S. aureus* growth in the presence of Hb as the sole iron source.
76 We also solved the crystallographic structure of Hb in complex with C35 to provide the basis
77 for chemical optimization of the compound. The structural analysis revealed a binding pose
78 different from the one initially hypothesized [12] but similar to that of a known class of
79 molecules which allosterically increase the affinity of Hb for oxygen by stabilizing its relaxed,
80 high-affinity state. These molecules are known as left shifters, as they shift the Hb oxygen
81 binding curve leftwards, i.e. to lower partial oxygen pressures. Under a pharmacological
82 perspective, the biological effect of left shifters is primarily exploited in the treatment of sickle
83 cell disease (SCD), where the stabilized state delays the polymerization of sickle Hb (HbS)
84 [13]. This finding prompted us to investigate the effect of C35 on increasing oxygen affinity
85 of Hb, a property that could confer an additional functional role to the molecule.

86 Results

87 C35 inhibits S. aureus growth in the presence of Hb as sole
88 iron source

89 In a recent study, we have identified a compound named C35 that binds Hb with high affinity
90 (K_D of 0.57 ± 0.06 μM) and interferes with the formation of the IsdB:Hb complex [12]. These
91 results suggested that C35 could act as a promising antimicrobial agent capable of
92 disrupting iron acquisition in *S. aureus*, thereby leading to bacterial iron starvation and
93 consequent growth inhibition. To investigate this hypothesis, a mutant lacking the IsdB
94 component of the Isd system was generated in *S. aureus* Newman (i.e., *S. aureus* Δ*isdB*).

95 Since the expression of the Isd system is regulated by the Ferric Uptake Regulator (Fur),
96 which enables its expression under iron-poor conditions, the chemically-defined medium
97 NRPMI devoid of iron was used [14]. To identify the best condition for C35-inhibitory testing,
98 we first investigated the role of Hb in supporting *S. aureus* growth in our experimental setting,
99 using both the WT and the Δ*isdB* strains. Bacteria were pre-cultured in RPMI supplemented
100 with 500 μM EDDHA, to iron-starve bacterial cells. The following day, cultures were sub-
101 inoculated in NRPMI in the presence of 500 μM EDDHA, supplemented or not with either
102 80 nM Hb or 500 μM $FeCl_3$, and monitored overtime for 96 h (Fig 1A). Results showed that
103 both strains failed to grow in the absence of an iron source, indicating that EDDHA, when
104 added at 500 μM, effectively prevents the acquisition of iron traces present in NRPMI, which
105 would likely occur through the production of siderophores, usually expressed under iron-
106 depleted conditions [15]. Interestingly, supplementation with 80 nM Hb promoted the growth
107 only of the WT strain but not of the Δ*isdB* (Fig 1A), in line with previous findings [6,14].
108 Notably, this Hb-mediated growth promotion was observed after 96 h post-incubation,
109 suggesting that *S. aureus* requires time to sense the presence of Hb in the medium, and
110 subsequently expresses the IsdB hemophore. In contrast, both strains were able to readily
111 utilize $FeCl_3$, showing comparable growth, thus confirming the specificity of IsdB for Hb
112 utilization (Fig 1A). Altogether, these data highlight the phenotypic characterization of the
113 Δ*isdB* mutant, thus providing a foundation for subsequent Hb-inhibitory testing.
114 C35 toxicity was investigated by monitoring the growth of WT and Δ*isdB* in NRPMI without
115 EDDHA, to allow bacterial growth, in the presence of different C35 concentrations (i.e., 1,
116 10 and 100 μM), and compared to the one of the positive control, devoid of the compound
117 (Fig 1B). No growth defect was observed for both strains at all C35 concentrations tested,
118 compared to the unamended controls (Fig 1B). Following the toxicity assessment of C35
119 towards *S. aureus*, the maximum concentration used (100 μM) was then selected to

120 investigate the ability of this compound to inhibit Hb-mediated growth promotion in the WT
121 strain. To this aim, *S. aureus* WT cells were cultivated in NRPMI supplemented with 500 μM
122 EDDHA and/or Hb, in the presence or absence of C35. Interestingly, C35 completely
123 inhibited the WT growth in the presence of 80 nM Hb as the sole iron source after 96 h post-
124 incubation, thus indicating that it is able to block IsdB-mediated Hb uptake in *S. aureus* (Fig
125 1C), while supplementation with 500 μM $FeCl_3$ as an alternative iron source, completely
126 abolished C35-mediated growth inhibition (Fig 1C). Additional evidence supporting the
127 proposed mechanism of action confirmed that C35 exerts its inhibitory effect by binding to
128 Hb, making it selective for the hemophore-mediated iron acquisition system. Indeed,
129 isothermal titration calorimetry (ITC) measurements excluded any measurable interaction
130 between C35 and IsdB at the tested concentrations (S1 Fig).

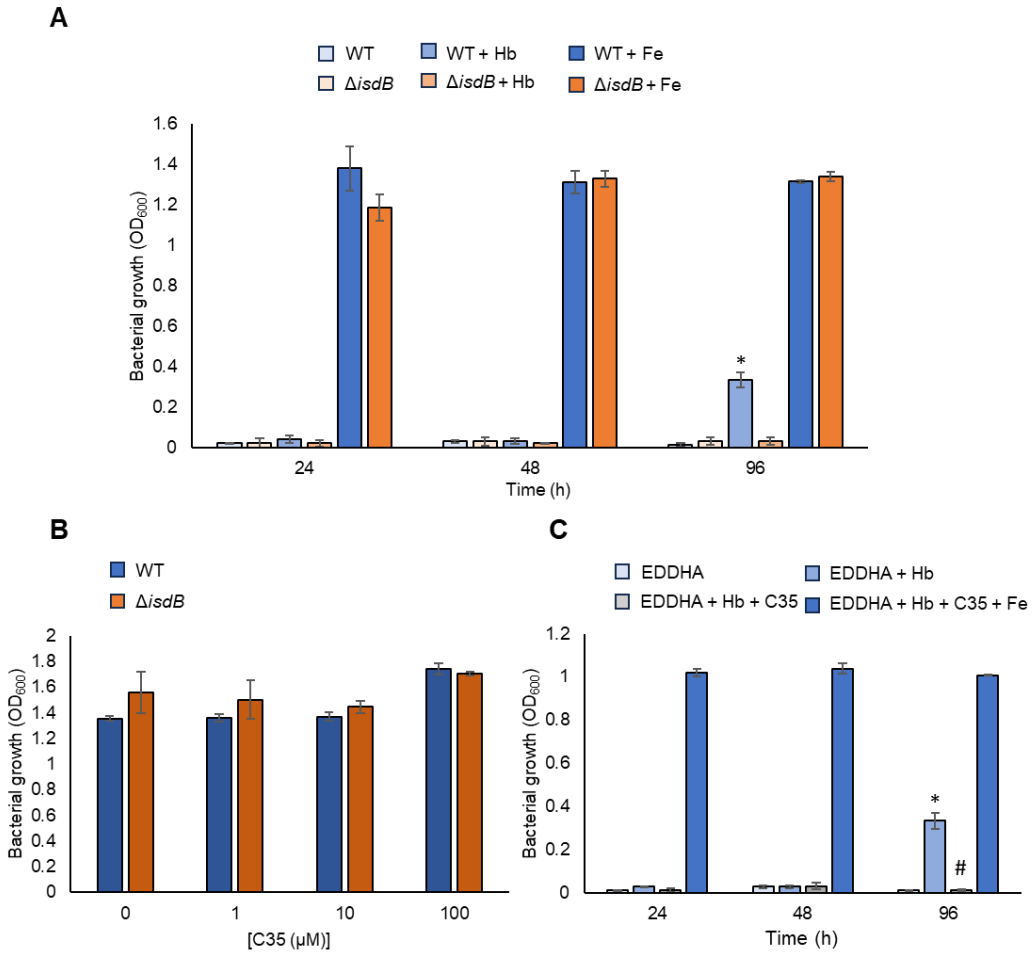

131

132 **Fig 1. C35 inhibits *S. aureus* growth in the presence of Hb as the sole iron source**. *S. aureus* WT and its
133 isogenic Δ*isdB* mutant were pre-cultured in RPMI supplemented with 500 μM EDDHA, to restrict iron
134 availability, for 16-20 h at 37 °C with good aeration (shaking 180 rpm). Next day, cultures were washed and
135 resuspended in NRPMI supplemented or not with the indicated compounds. (A) Effect of 80 nM Hb (Hb) and
136 500 μM $FeCl_3$ (Fe) on *S. aureus* WT and Δ*isdB* growth, in RPMI + 500 μM EDDHA; (B) Toxicity of C35 on *S.*
137 *aureus* WT and Δ*isdB*, grown for 24 h in NRPMI without EDDHA, to allow the growth of both strains; (C) Effect
138 of 100 μM C35 on *S. aureus* WT grown in NRPMI + 500 μM EDDHA (EDDHA) supplemented with 80 nM Hb
139 alone or in combination with 500 μM $FeCl_3$. As negative control, the growth of the WT strain in NRPMI + 500
140 μM EDDHA was also included. Each value is the average of three different cultures ± standard deviation. The
141 symbols indicate statistically significant differences as determined by a Student's t test ($P < 0.05$) in relation to
142 the WT strain grown in the presence of EDDHA with no Hb (*) or the WT strain grown in the presence of
143 EDDHA with Hb (#).

144

145 Three-dimensional structure of Hb-C35 complex

146 Given the ability of C35 of inhibiting *S. aureus* growth and aiming to further explore this
147 molecule as a potential lead compound, we decided to investigate the binding of C35 to Hb
148 at atomic resolution. The X-ray crystallographic structure of tetrameric Hb in complex with
149 C35 was obtained by co-crystallization (PDB ID: 9HBA and Fig 2A). The final resolution was
150 1.5 Å and the crystals form showed a symmetry belonging to the space group P 32 2 1.

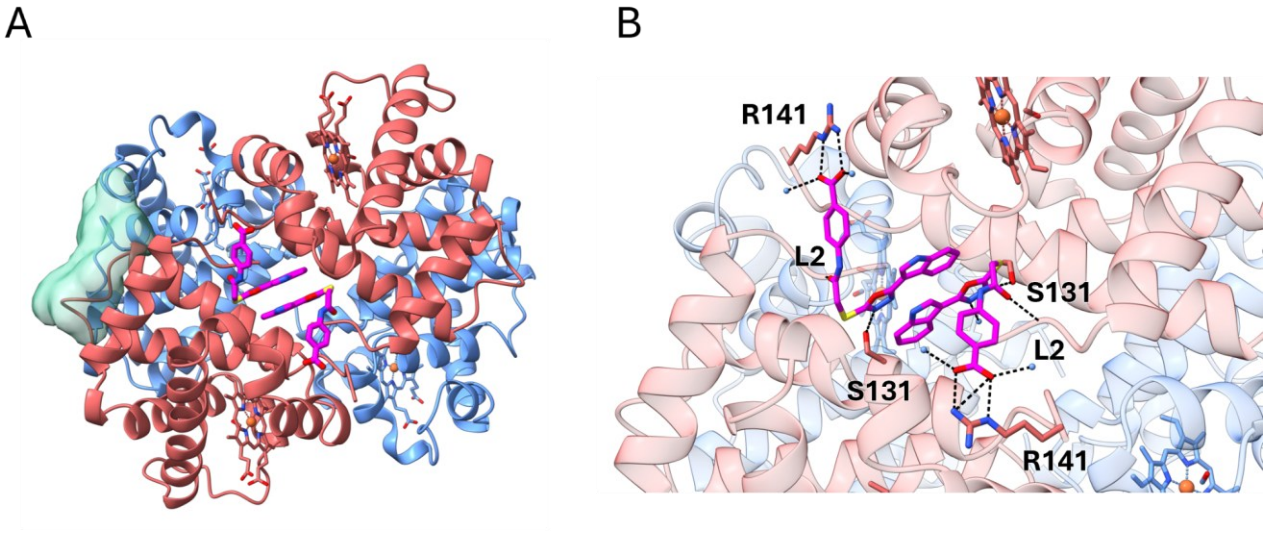

Fig 2. **Binding of C35 to Hb.** (**A)** The X-ray three-dimensional structure of Hb co-crystallized with the compound C35. Alpha subunits and beta subunits are shown as red and blue ribbons, respectively; the green surface represents the putative binding site of C35 as predicted by molecular docking [12]; C35 is shown in magenta. **(B)** Close-up of the binding site of C35 in the cleft between the two Hb alpha subunits (in red). Beta subunits are in blue, C35 in magenta, while contacts are shown as black dashed lines. Water molecules are represented as light blue spheres.

The binding stoichiometry of C35 to Hb observed in the crystals is 2:1, i.e. two molecules of C35 symmetrically bind one Hb tetramer, confirming the stoichiometry estimated by ITC [12]. However, the crystallographic structure identified a binding pocket that differs from the one proposed by docking in our recent paper [12] (Fig 2A). Indeed, the obtained structure shows C35 bound in a cleft between the Hb alpha subunits. In this pocket, the two C35 molecules form several symmetrical interactions with Hb alpha lining residues (Fig 2B). Specifically, the benzoic acid moiety of each C35 molecule interacts through a salt bridge with the positively charged lateral chain of Arg141. Each molecule of C35 establishes an H-bond between the oxadiazolic moiety and the side chain of Ser131 (helix H) and another H-bond between the amide group of C35 and the -NH on the backbone of Leu2. The oxadiazolic

169 and the indolic moieties of both C35 molecules interact with each other through a stacking
170 interaction. Furthermore, being the C35 binding site partially exposed to the solvent, different
171 polar contacts with water molecules are also observed.

172 C35 binds Hb in the same cleft of Hb left shifters and stabilizes
173 a R2 conformation

174 Structural analysis of the Hb-C35 complex uncovered a previously unreported binding site
175 for C35. To further investigate this new finding, we conducted a detailed comparison of Hb
176 in complex with C35 with the structures of Hb deposited in the PDB.

177 This analysis was performed using the ''Structure similarity search'' tool available on the
178 PDB website (https://www.rcsb.org/search/advanced/structure). The tool performs a
179 comprehensive analysis of the PDB, taking into account the entire protein assembly,
180 including its ternary/quaternary state and any bound molecules. The first ten structures
181 returned by the algorithm are listed in S2 Table and are all human Hb structures in the R
182 conformation. The R state corresponds to a conformation of Hb with high oxygen affinity,
183 where the α1β1 dimer is rotated by 15° with respect to the α2β2 dimer compared to the low
184 oxygen affinity T state. Among the top 5 highest-scoring structures, two presented a ligand
185 bound in a similar position with respect to C35 (i.e., PDB ID: 1QXE and PDB ID: 3IC0). In
186 1QXE Hb binds a molecule of 5-hydroxymethyl furfural (5-HMF) and in 3IC0 a derivative of
187 vanillin (INN298). Both molecules were characterized by Safo's group as Hb left-shifters
188 [16,17], i.e., ligands that stabilize the R state with respect to the T state, thus increasing the
189 oxygen affinity. These molecules have been developed as potential therapeutic agents
190 against sickle cell anemia.

191 This finding raised the question of whether C35 might share similar properties and mode of
192 action with those compounds. We focused on the comparison between C35 and INN298 (4-

193 hydroxy-3-methoxybenzaldehyde), a more potent Hb left-shifter than 5-HMF (Fig 3A and Fig
194 3B).

195 INN298 and C35 share the same binding site on Hb (Figs 3C and 3D), although some
196 differences are present. First, the binding stoichiometry of C35 is 2:1 (on tetramer base, *vide*
197 *supra*), while the stoichiometry for INN298 is 4:1, with two of the four molecules forming a
198 covalent bond with the terminal amino group of Val1 in the alpha chains, while the other two
199 interact through non-covalent bonds. Differently from INN298, C35 only binds Hb *via* non-
200 covalent interactions.

201 It is well known that compounds able to interact with Hb in the allosteric binding site between
202 the alpha subunits can stabilize a relaxed R conformation. In particular, INN298 stabilizes
203 an alternative quaternary Hb conformation named R2 state, over the R state trajectory
204 [18,19]. The R and R2 states of tetrameric Hb mainly differ in the positioning of the α2β2
205 dimer relative to the α1β1 dimer. Therefore, to investigate the effect of C35 on the Hb
206 quaternary structure, we compared C35-bound Hb with reference structures by calculating
207 the global root mean square deviation (RMSD) on the α2β2 subunits after superimposing
208 the α1β1 subunits. As references, we used R-state HbCO (PDB ID: 2DN3, [20]) and R2-
209 state Hb bound to INN298 (PDB ID: 3IC0) (Fig 3E). The RMSD calculated relative to the R2
210 structure stabilized by INN298 is very low (0.54 Å) compared to that obtained relative to the
211 R structure (4.39 Å). This result suggests that C35, similarly to INN298, can stabilize an R2
212 Hb conformation.

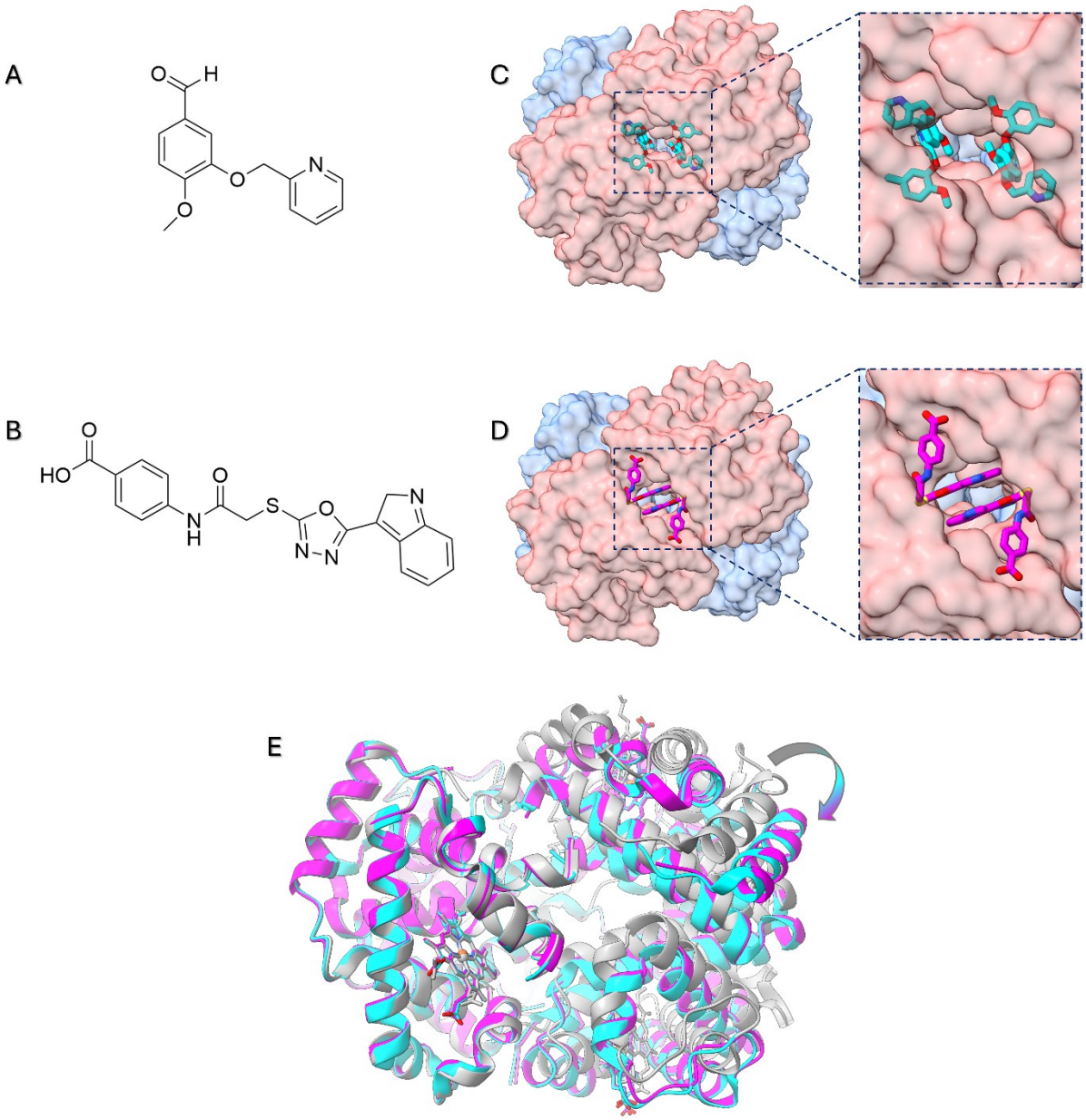

Fig 3. **Structural comparison between Hb bound to C35 and Hb bound to INN298.** (A) Chemical structure of the compound INN298. (B) Chemical structure of the compound C35. (C) Molecular surface of Hb bound to INN298 and its close-up on the INN298 binding site. (D) Molecular surface of Hb bound to C35 and its close-up on C35 binding site (PDB ID: 9HBA). INN298 and C35 are reported as cyan and magenta sticks, respectively. (E) Superimposition of the alpha-1 and beta-1 chains of different tetrameric Hb structures: HbCO (R state, PDB ID: 2DN3 – grey ribbons), Hb bound to INN298 (R2 state, PDB ID: 3IC0 – cyan ribbons) and Hb bound to C35 (R2 state, PDB ID: 9HBA – magenta ribbons). Heme molecules are represented as sticks. The

221 RMSD values estimated for Hb bound to INN298 or to C35 considering R-state Hb as a reference are 4.46 Å
222 and 4.39 Å, respectively. The RMSD value between INN298- and C35-bound Hbs is 0.54 Å.

223

224 Compound C35 increases Hb oxygen affinity

225 Considering that C35 and the left-shifter INN298 share the same binding site and induce
226 comparable changes in Hb structure, we decided to compare the effect of the two molecules
227 on the functional properties of Hb, i.e., on its oxygen binding affinity and cooperativity.

228 INN298, stabilizing the R conformation, reduces the binding cooperativity of oxygen to Hb
229 and increases the oxygen affinity, thus also slowing down the HbS polymerization process
230 that involves the deoxy form of the protein [13,17]. However, in the reference study [17], the
231 effect of INN298 on oxygen binding was only investigated in intact RBCs, where, in addition
232 to its direct action on Hb, the permeation of the effector into the cells must also be
233 considered. Here, we decided to investigate the activity of INN298 at the highest
234 concentration tested in [17] (i.e., 2 mM).

235 The reference oxygen binding curve of Hb showed a *p*50 of 8.1 ± 0.3 torr, with a Hill
236 coefficient (n) of 1.9 ± 0.1 (Fig 4 and Table 1). Stripped Hb (i.e., Hb outside RBCs in the
237 absence of any allosteric effector) has a reported n of approximately 2.4 [21]. The lower
238 value measured here is likely due to the effect of DMSO (used at a concentration of 2% (v/v)
239 to align with studies conducted with INN298 and C35), as reported in the work of Liu and
240 colleagues [22]. As expected, INN298 shifted to the left the oxygen binding curve of Hb, with
241 a *p*50 value of 0.8 ± 0.1 torr in the presence of the compound (Fig 4 and Table 1). Also,
242 cooperativity was found to be strongly affected by the presence of INN298, with a Hill
243 coefficient dropping to 0.8 ± 0.1.

244 The oxygen binding curve in the presence of C35 was measured at a final concentration of
245 1 mM compound. This concentration is significantly higher than its dissociation constant (K_D
246 = 0.57 ± 0.06 μM, [12]) but was necessary to saturate Hb, which was present at a
247 concentration of 100 μM in the analysis to allow monitoring of the absorption of Q bands for
248 the calculation of the fractional saturation (Fig 4A and 4B). The p50 calculated in the
249 presence of C35 was 1.2 ± 0.1 torr (Fig 4C and Table 1), almost comparable to the value
250 obtained in the presence of INN298. Also in this case, the cooperativity of oxygen binding is
251 almost completely lost, with a Hill coefficient of about 1.2 ± 0.1 (Fig 4C and Table 1).

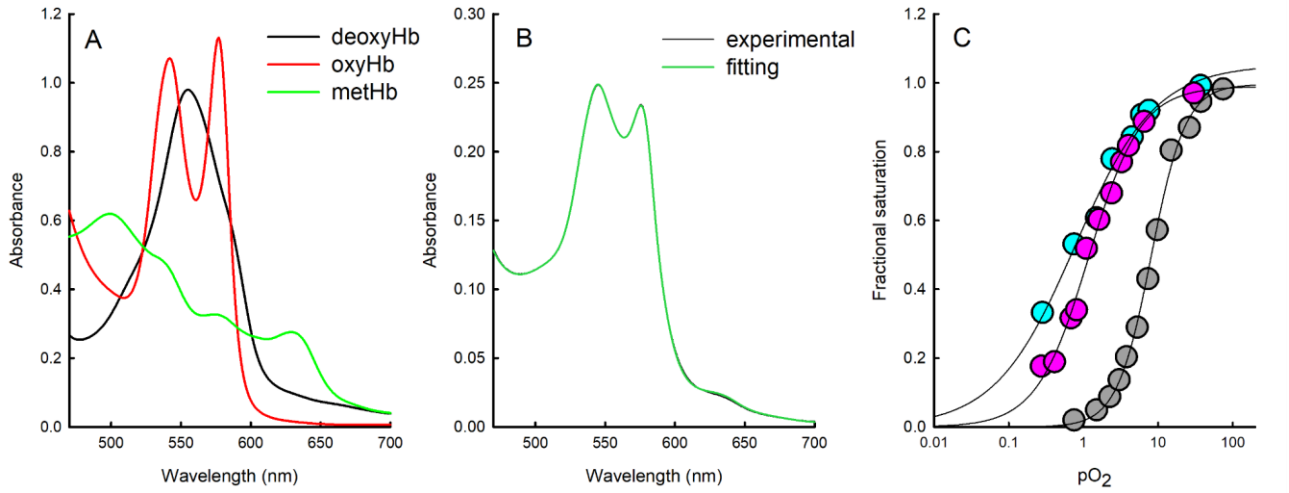

252

253 **Fig 4. Effect of C35 and INN298 on the oxygen binding to Hb.** (A) Reference spectra used for linear
254 combination. (B) Example of comparison between an experimental spectrum (black line) measured at a pO2
255 of 9.4 torr and the corresponding fit to the linear combination of reference spectra (green line). (C) Oxygen
256 binding curves of Hb measured at 37 °C in the absence (grey circles) and presence of either 1 mM C35
257 (magenta circles) or 2 mM INN298 (cyan circles). The data points represent the Hb fractional saturation with
258 oxygen obtained from linear combination of reference spectra. Lines through data points are the fitting to the
259 Hill equation (Eq. 3). The estimated values are reported in Table 1.

260

261 **Table 1**. ***p*50 and Hill coefficient of Hb in the absence and presence of either 2 mM INN298 or 1 mM C35**
262 **at pH 7.4, 37 °C.**

	Ref	**+ 2 mM INN298**	**+ 1 mM C35**
p_{50} (torr)	8.1 ± 0.3	0.8 ± 0.1	1.2 ± 0.1
n (Hill)	1.9 ± 0.1	0.8 ± 0.1	1.2 ± 0.1

263

264 C35 does not impair haptoglobin binding to Hb

265 In the crystal structure of tetrameric Hb with C35, the compound binds at the interface
266 between the two Hb dimers, specifically at the level of the alpha subunits. Under
267 physiological conditions, haptoglobin (Hp) binds free Hb dimers in the bloodstream *via*
268 specific non-covalent interactions, forming a stable complex that prevents renal loss and
269 oxidative damage by enabling Hb clearance through CD163-expressing macrophages [23].
270 During the initial virtual screening campaign, C35 was selected to interact with a region of
271 Hb that would not interfere with Hp binding [12]. However, in its newly identified binding pose
272 revealed by the crystal structure, the position of C35 is apparently not compatible with the
273 co-presence of Hp bound to a Hb dimer. In fact, the structural alignment of a single Hb dimer
274 bound to two C35 molecules (from the crystal structure of tetrameric Hb with C35) with the
275 crystal structure of the Hb:Hp complex shows that C35 occupies a region involved in Hb:Hp
276 interaction interface (Fig 5A). This observation prompted us to experimentally investigate
277 whether C35 might affect Hb:Hp complex formation, as this potential interference would
278 represent a serious limitation for the compound's further development as a pharmacological
279 candidate, either as antibiotic or Hb left-shifter.

280 To explore the effect of C35 on Hb:Hp interaction, we performed SEC experiments. As a
281 first step, experimental conditions were optimized to isolate the Hb:Hp complex
282 chromatographically. Hb and Hp were mixed in solution at a 2:1 stoichiometric ratio (one Hb
283 dimer per Hp protomer), and the resulting chromatogram was compared to those of the
284 individual proteins run separately (Fig 5B). The chromatogram of the Hb-Hp mixture showed
285 a single peak with a lower elution volume (1.19 mL) than each of the separate proteins (1.22
286 mL for Hp and 1.61 mL for Hb), indicating the formation of a higher molecular weight
287 complex. Moreover, no residual peaks corresponding to the individual proteins were
288 observed for the 2:1 Hb:Hp sample, confirming that the complex had been successfully
289 isolated.

290 Maintaining the same protein concentrations and stoichiometry, we repeated the SEC
291 experiment in the presence of C35, added at a concentration of 1 mM to both the sample
292 and the mobile phase. While the resulting chromatographic peak appeared slightly broader
293 compared to the control, the elution volume remained unchanged, and no additional peaks
294 corresponding to unbound Hb or Hp were detected. These observations indicate that C35
295 does not disrupt the Hb:Hp complex under the tested conditions. Accordingly, no off-target
296 effects related to Hb:Hp dissociation are expected for this compound.

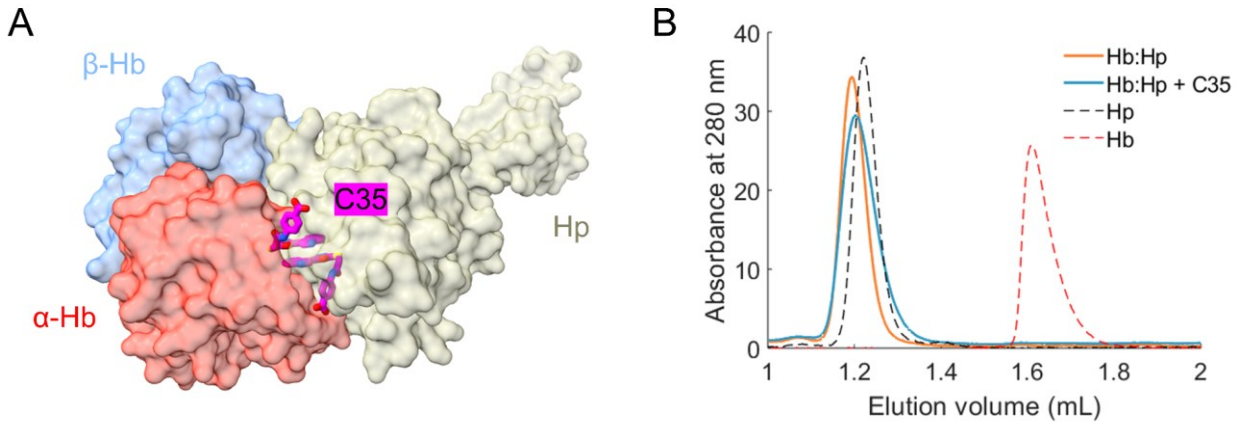

297

298 **Fig 5**. **Effect of C35 binding on the formation of the Hb:Hp complex.** (A) Comparison of the binding mode
299 of C35 and Hp on a Hb dimer. A single Hb dimer of the crystal structure obtained in this study (PDB ID: 9HBA)
300 was aligned with the structure of the Hb:Hp complex (PDB ID: 4F4O). Protein surfaces are shown as semi-
301 transparent: Hb α-chains in red, Hb β-chains in blue, and a single Hp protomer (α- and β-chains) in yellow.
302 C35 is shown as magenta sticks. (B) SEC profiles of isolated Hb (red dashed line) and Hp (black dashed line),
303 and of the Hb:Hp complex (2:1 molar ratio; one Hb dimer per Hp protomer) in the absence (orange line) and
304 presence (blue line) of 1 mM C35.

305

306 # Discussion

307 In this work, we report the serendipitous identification of the small molecule C35 as a dual-
308 function compound: an allosteric effector of Hb that increases its oxygen affinity, and a
309 potent antimicrobial agent that inhibits *S. aureus* growth by interfering with iron acquisition.
310 Originally selected for its ability to disrupt the Hb:IsdB interaction *in vitro*, C35 was shown to
311 effectively inhibit *S. aureus* growth under iron-limited conditions, an effect that was reversed
312 by excess of $FeCl_3$, strongly suggesting iron starvation as the underlying antibacterial
313 mechanism.

314 Structural studies revealed that C35 binds in a solvent-exposed cleft between the α-subunits
315 of the Hb tetramer, a site shared with known Hb left-shifters such as INN298 [17] and
316 Voxelotor [24]. This binding mode, distinct from the originally predicted docking pose,
317 stabilizes an R2 quaternary conformation of Hb, characterized by high oxygen affinity and
318 reduced cooperativity. Unlike most known left-shifters, which form covalent adducts with Hb,
319 C35 interacts *via* non-covalent forces, representing a prototype molecule for a novel class
320 of Hb modulators. Notably, this binding mode is, to date, shared only by PF-07059013, a
321 non-covalent Hb left-shifter that recently entered clinical phase 1 trials and exhibits a similar
322 interaction interface with nanomolar affinity for Hb

323 (https://clinicaltrials.gov/study/NCT04323124). This convergence further underscores the
324 growing pharmacological interest in non-covalent Hb modulators as safer and potentially
325 more tunable therapeutic alternatives.

326 The inhibition of *S. aureus* growth in the presence of C35 raised the question of whether this
327 activity could be linked to altered Hb oligomerization dynamics. Specifically, since heme
328 extraction by the Isd system requires Hb dimerization [25], it was hypothesized that C35
329 may exert its inhibitory effect by stabilizing the tetrameric form of Hb, thereby limiting the
330 accessibility of heme to IsdB. However, experimental analysis by SEC demonstrated that
331 C35 does not significantly affect the tetramer-to-dimer equilibrium of Hb (S2 Fig), suggesting
332 that the primary mechanism of action is not related to oligomeric stabilization but rather to
333 direct competition with hemophore binding *via* conformational effects or steric hindrance.

334 It should be noted that Hb is expected to be mostly in the dimeric state at the concentrations
335 used for the ELISA that was employed for the initial screening [12] and the *S. aureus* growth
336 inhibition assay presented here. This hints to the possibility of C35 binding to the Hb dimer
337 with a different (or a further) binding pose with respect to that observed for the tetramer in
338 crystallographic experiments. The fact that Hb concentrations required for crystallization
339 shift the dimer-tetramer equilibrium towards the latter hampers further investigation by
340 crystallographic techniques.

341 To our knowledge, this is the first demonstration that a single ligand can simultaneously
342 modulate oxygen binding to Hb, through the stabilization of a specific Hb quaternary
343 structure, and interfere with heme scavenging by bacterial hemophores. This discovery
344 opens new avenues for the development of dual-acting compounds that target both the
345 functional modulation of Hb and bacterial iron acquisition. Rational design strategies could
346 exploit C35's scaffold to generate derivatives with controlled RBC permeability: cell-

347 permeable analogs might serve as Hb left-shifters for the treatment of SCD, while
348 impermeable variants could function extracellularly as antimicrobials during systemic
349 infections. In terms of antimicrobial activity, moreover, it is worth noting that several bacterial
350 iron acquisition systems rely on heme extraction from Hb [26,27]. Given that C35 exerts its
351 effect through direct binding to Hb, it is conceivable that it could interfere with other bacterial
352 iron acquisition systems that similarly exploit heme scavenging from host sources.

353 The clinical relevance of such dual-acting agents is underscored by the increased
354 susceptibility of SCD patients to bacterial infections [28]. For this population, bifunctional
355 C35 derivatives with balanced intra- and extracellular distribution could simultaneously
356 address both pathological Hb polymerization and the associated infectious risk. Although
357 the concentrations required to modulate intracellular and extracellular targets may differ
358 substantially, it can be speculated that compounds favoring RBC uptake might still retain
359 sufficient plasma levels to exert antibacterial activity, thereby offering a dual therapeutic
360 benefit even with a predominant intracellular partitioning.

361 In conclusion, our study highlights the therapeutic potential of targeting the α-subunit
362 interface of Hb as a novel pharmacological hotspot, offering a promising platform for the
363 development of compounds that combine hemoglobinopathy treatment with antimicrobial
364 action.

365

366 Materials and Methods

367 Chemicals and solubilization of C35

368 All reagents were purchased by MERCK (St. Louis, MO, USA) and were used as received.
369 C35 was synthesized in-house, with a purity of at least 95%, as reported in [12] (see

370 Scheme) and dissolved in 100% dimethyl sulfoxide (DMSO, Sigma-Aldrich) at a final
371 concentration of 100 mM.

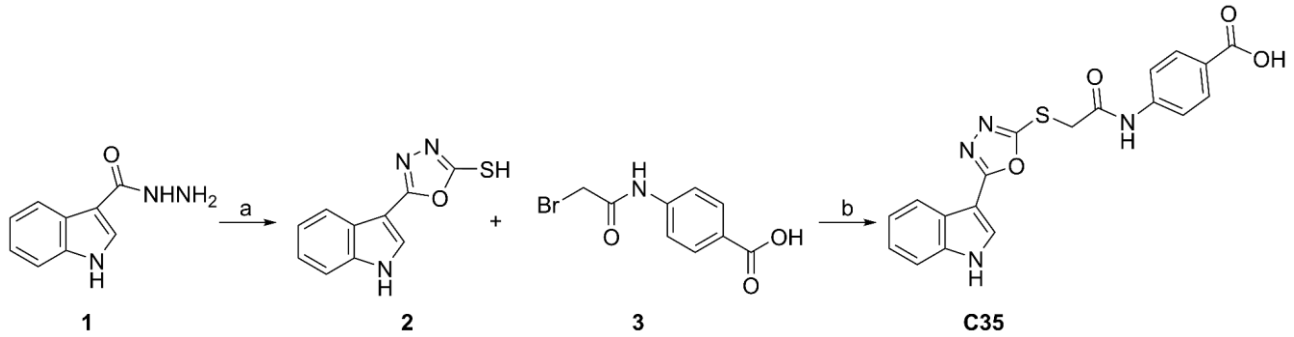

372
373
374 a) KOH, CS_2, EtOH, reflux, 4 h. b) K_2CO_3, acetone reflux
375

376 Bacterial strains and growth conditions

377 All experiments were carried out with *S. aureus* strain Newman [29] and its isogenic in frame-
378 deletion mutant strain (Δ*isdB*). The Δ*isdB* mutant was obtained following the mutagenesis
379 protocol described in Schuster et al. [30]. For inactivation of the *isdB* gene, a 955-bp
380 fragment and a 989-bp fragment overlapping ATG and the TAA of *isdB*, respectively, were
381 amplified by PCR using the primer couples UPFW*isdB*: 5'-
382 AACTGCAGCCAAACCGTGTTAAACAATG-3'/UPRVi*sdB*: 5'-
383 CCCAAGCTTGTTCATGTTGTAGAAACAAC-3' and DWFW*isdB*: 5'-
384 CCCAAGCTTAACTAATAAATCGTCTTTATATTT-3'/DWRV*isdB*:5'-
385 CCGCTCGAGTGCTAGATTCACAAACGG-3', respectively, and cloned in pIMAY*, yielding
386 pIMAY*Δ*isdB*. Then, the latter was introduced by electroporation into *S. aureus* wild type.
387 The functionality of the plasmid was then examined using a temperature-sensitivity test,
388 confirming the ratio of colonies on plates incubated at 28 °C and 37 °C. Chromosomal
389 integration *via* a single crossover event was achieved by incubating *S. aureus/*pIMAY*Δ*isdB*
390 transformants at 37 °C with antibiotic selection and verifying by a colony PCR using the

391 T3/T7 primers. The second crossing-over event was encouraged by culturing/sub-culturing
392 the selected clones at 28 °C for at least 50 generations, followed by verification of plasmid
393 loss using para-chlorophenylalanine (PCPA), a toxic phenylalanine analogue. Once
394 chloramphenicol sensitivity was confirmed, genomic DNA was extracted from potential
395 candidates and the deletion was confirmed by PCR using primers OUTFW*isdB*: 5'-
396 TGTATACATAGGCGCAGACA-3')/OUTRV*isdB*: 5'-AACTCGCGGTCTATTGCCA-3', and
397 PCR fragments were checked by sequencing.

398 Bacterial strains were routinely cultured in Tryptic Soy Agar (TSA) at 37 °C for 18 h and
399 stored with 15% glycerol (v/v) at -80 °C. In this study, two media were used: *i)* Roswell Park
400 Memorial Institute (RPMI-1640, Sigma-Aldrich) broth prepared according to the
401 manufacturer's instructions with a modification; RPMI was supplemented with 1% casamino
402 acids (CAA) (w/v) to support bacterial growth, and *ii)* metal-depleted RPMI (NRPMI)
403 prepared following the protocol described by Pishchany et al. [14]. Briefly, the RPMI medium
404 was treated for 16 h at 4 °C with 70 g/L of the metal-chelating Chelex® resin (Bio-Rad) under
405 moderate stirring, then filtered through Whatman no. 1 filter paper. The medium was
406 subsequently supplemented with non-iron metals: 25 μM $ZnCl_2$, 25 μM $MnCl_2$, 100 μM $CaCl_2$
407 and 1 mM $MgCl_2$ prepared in advance as sterile 1,000x solutions. The pH of the NRPMI was
408 then adjusted to 7.4, then sterilized by filtration using Corning® filter system (Corning) and
409 stored at 4 °C.

410 When required, ethylenediamine-N,N'-bis(2-hydroxyphenylacetic acid) (EDDHA) was
411 resuspended in anhydrous ethanol to a final concentration of 100 mM for sterilization, and
412 then added to the culture medium at the required concentration. $FeCl_3$ (Sigma-Aldrich) was
413 prepared as a 0.1 M stock solution in 10 mM HCl and stored at -20 °C. A stock solution of
414 930 μM human Hb (see below) was prepared and stored at -80 °C in phosphate-buffered

415 saline (PBS). For C35, a 100 mM stock solution was freshly prepared in DMSO and stored
416 at -20 °C.

417 The ability of *S. aureus* WT and its isogenic Δ*isdB* to grow in NRPMI was investigated by
418 monitoring bacterial growth (OD_{600}) over time, as described in Pishchany et al. [14]. For that,
419 *S. aureus* WT and its isogenic Δ*isdB* mutant were pre-cultured in RPMI supplemented with
420 500 μM EDDHA, to restrict iron availability, for 16-20 h at 37 °C with 180 rpm shaking. The
421 next day, cultures were centrifuged for 5 min at 7,500 *x g* and the pellets were resuspended
422 in NRPMI containing 500 μM EDDHA and normalized to OD_{600} = 3. 10 μL of bacterial
423 suspension were subcultured into 1 mL NRPMI in a 15 ml screw-cap conical tube,
424 supplemented with either 500 μM EDDHA and/or 80 nM Hb and/or 100 μM C35, and
425 incubated at 37 °C with vigorous shaking. Bacterial growth (OD_{600}) was measured in a
426 multiplate reader (SPARK 10M TECAN®) every 6-12 h for up to 96 h.

427 Protein purification

428 Human hemoglobin A (Hb) was purified from outdated blood donated by non-smoking
429 volunteers to a blood transfusion center, following the procedure described in Viappiani et
430 al. [31]. Written informed consent was obtained from all donors, and both the blood donation
431 and the use of outdated samples complied with Italian law 219/2005 on blood donation and
432 usage. RBCs were washed with saline and lysed under hypotonic conditions by adding
433 seven volumes of Buffer Hb1 (10 mM HEPES pH 6.9, 1 mM EDTA). The lysate was clarified
434 by centrifugation (23,000 *x g*, 1 h, 4 °C), and the supernatant containing oxygenated Hb was
435 dialyzed against Buffer Hb1. The sample was then loaded onto a CM-Sephadex C-50
436 column (100 × 5 cm). Soluble RBC components were separated from Hb using a linear
437 gradient from 0% to 80% Buffer Hb2 (10 mM HEPES pH 8.6, 1 mM EDTA); Hb was
438 subsequently eluted using a gradient from 80% to 85% Buffer Hb2. The purified Hb was

439 dialyzed into storage buffer (10 mM HEPES pH 7.2, 1 mM EDTA), aliquoted, flash-frozen in
440 liquid nitrogen, and stored at −80 °C. The concentration and oxidation state of oxyHb were
441 assessed by UV–Vis absorption spectroscopy using known molar extinction coefficients for
442 heme-specific absorbance peaks [32].

443 Strep-tagged IsdB was expressed and purified as described previously [33]. Strep-tag® II-
444 IsdB (residues 125–485, UniProt Q8NX66) was codon-optimized for *Escherichia coli*, cloned
445 into pASK-IBA3-plus vector, and expressed in *E. coli* BL21 strain induced with 0.2 µg/mL
446 anhydrotetracycline at 20 °C for 20 h. Cells were lysed, and the protein purified using Strep-
447 Tactin®XT affinity resin followed by SEC in Buffer W. Final yield exceeded 100 mg/L with
448 >95% purity. Protein concentration was calculated using ε_{280nm} = 47,790 M^{-1} cm^{-1}, with holo-
449 IsdB content estimated to be <5% based on heme absorbance at 405 nm (ε_{405nm} =
450 90,500 M^{-1} cm^{-1}) [33].

451 Hb co-crystallization with C35

452 Crystals of carboxyhemoglobin (HbCO) grew in the presence of 10 mM C35 in a solution
453 containing 3.0 M ammonium sulfate and 1% (w/v) 2-methyl-2,4-pentanediol (MPD) in sitting
454 drop conditions after which the crystals were cryo-cooled in liquid nitrogen for data
455 collection. X-ray diffraction data was collected at Diamond Light Source beamline i03 at
456 wavelength 0.9763Å. Data was integrated and scaled using the CCP4 package; structures
457 were solved by molecular replacement using Phaser crystallographic software [34]. The
458 structural model was iteratively refined and rebuilt by using the Coot program [35]. Ligand
459 coordinates and restraints were generated from the SMILES string using the Grade software
460 package (Global Phasing Ltd). The structure coordinates are deposited on Protein Data
461 Bank (PDB) (9HBA), and the data collection and refinement statistics are shown in S1 Table.

462 To investigate the presence of global 3D-shape similarity, using the C35-bound Hb as a
463 reference, the ''Structure similarity search'' tool on the PDB website
464 (https://www.rcsb.org/search/advanced/structure) was exploited. The search was
465 conducted by uploading the C35-bound Hb structure in pdb format without relaxation step
466 and considering only molecular assemblies.

467 Oxygen binding to Hb

468 Oxygen-binding curves of 100 μM Hb were measured with a modified tonometer [36] in 100
469 mM HEPES, 1 mM EDTA, pH 7.4 at 37 ± 0.4 °C in either the presence or absence of studied
470 effectors. The oxygenated Hb (oxyHb) concentration was estimated using the extinction
471 coefficient at 415 nm of 125,000 M^{-1} cm^{-1}. The Hayashi reducing system was exploited to
472 prevent autoxidation [37] during measurements. Before measurement, oxyHb was
473 deoxygenated under helium (50 mL/min) for 60 minutes to obtain the deoxygenated form
474 (deoxyHb). Samples were then exposed to different partial oxygen pressures (pO_2),
475 generated using an Environics 4000 gas mixer (Environics Inc, Tolland, CT, U.S.A.),
476 connected to a helium bottle and different premixed helium/oxygen bottles. Spectra were
477 collected after 30 minutes incubation time in the 450–700 nm range using a Cary 4000
478 spectrophotometer (Agilent, Santa Clara, CA, USA). The control experiments, performed in
479 the absence of any ligands, were carried out in the presence of 2% DMSO (v/v).

480 The Hb fractional saturation at each pO_2 was calculated by adapting the method reported
481 by Rivetti et al. [38]. Spectra were analyzed as a linear combination of the deoxyHb, oxyHb
482 and metHb spectra (i.e., the reference spectra) measured under the same experimental
483 conditions (Eq. 1):

484 $$S = S_0 + a \sum_i f_i S_i$$

485 Where S is the measured absorbance spectrum, S_0 is an offset, a is the scale factor to
486 correct for the intensity of the analyzed spectrum, the index i denotes the heme species
487 (oxyheme, deoxyheme and metheme), S_i are the reference spectra and f_i are the fractional
488 coefficients. The estimation of the oxygen saturation (y) is obtained as (Eq. 2):

489 $$y = \frac{f_{oxy}}{f_{oxy} + f_{deoxy}}$$

490 The pO_2 corresponding to 50% fractional saturation (p50) and the Hill coefficient (n) were
491 estimated by fitting the calculated fractional saturation at different pO_2s to the Hill equation
492 (Eq. 3):

493 $$y = \frac{{pO_2}^n}{{p_{50}}^n + {pO_2}^n}$$

494 Where y is the oxygen saturation, a is the amplitude, x is the pO_2, p50 is the oxygen partial
495 pressure corresponding to 0.5 fractional saturation and n is the Hill coefficient, accounting
496 for binding cooperativity.

497 Isothermal Titration Calorimetry

498 Experiments were performed at 25 °C using 12 μM IsdB and 1 mM C35 in a buffered
499 solution containing 50 mM HEPES buffer, pH 7.6. C35 was first dissolved at 100 mM in
500 DMSO and then diluted in the final buffer to a concentration of 1 mM. Solutions were
501 degassed for 10 min under vacuum before the titration. DMSO was added to the IsdB
502 solution at a final concentration of 1% to balance the amount of DMSO in the C35 solution.
503 ITC titrations were carried out using a MicroCal PEAQ-ITC instrument (Malvern, Malvern,
504 UK). C35 was added to the instrument measurement cell, containing 280 μL of IsdB, by a
505 first addition of 0.4 μL and 18 subsequent additions of 2 μL. A time interval of 150 s was set
506 between the addition of each aliquot of C35. To subtract the dilution heat, a reference

507 experiment was performed in which the reaction cell was filled only with the buffer solution
508 with 1% DMSO, while the syringe was filled with 1 mM C35. Experiments were performed
509 under continuous stirring at 750 rpm. All experiments were performed in triplicate. Data
510 analysis was performed using MicroCal PEAQ-ITC Analysis Software (version 1.41, Malvern
511 Panalytical, Malvern, UK).

512 Size-exclusion chromatography

513 SEC was performed to assess whether compound C35 exerts a destabilizing effect on the
514 Hb:haptoglobin (Hb:Hp) complex and/or on the quaternary structure of isolated Hb (i.e., its
515 tetrameric form).

516 The destabilizing effect of compound C35 on the Hb:Hp complex was investigated by
517 exploiting an Agilent 1260 HPLC system (Agilent Technologies, Inc., Santa Clara, CA, USA)
518 equipped with a Superdex® 200 Increase 3.2/300 column (Cytiva). The column was pre-
519 equilibrated with PBS buffer (pH 7.4) either in the absence or presence of 1 mM C35, and
520 operated at a flow rate of 0.07 mL/min. Samples containing Hb, Hp (Phenotype 1-1) or the
521 Hb:Hp complex (prepared using a 2:1 stoichiometry, i.e., one Hb dimer associated with one
522 Hp protomer), at concentrations of 2 mg/mL, were injected and eluted at 25 °C. Elution
523 profiles were monitored by measuring absorbance at 280 nm and 406 nm using an Agilent
524 1260 Infinity II WR Diode Array Detector.

525 The estimation of the dissociation constant for the Hb dimer/tetramer equilibrium was carried
526 out using an ÄKTA Pure 25 M chromatographic system (GE Health Sciences™, Chicago,
527 IL, USA) equipped with a Superdex 75 Increase 5/150 GL column (GE Health Sciences™)
528 with a mobile phase consisting of 20 mM Tris, 150 mM NaCl and 1 mM EDTA pH 8.0 at 20
529 °C, either in the absence or presence of 0.01 mM C35. Control experiments in the absence
530 of C35 were carried out adding 0.01% (v/v) DMSO. The amount of DMSO in the control

experiments accounts for the same amount of DMSO related to C35-treated samples. The flow rate was set to 0.3 mL/min. The separation was run at room temperature and the absorbance of the column effluent was monitored both at 280 nm (for calibration) and to 415 nm (for Hb samples). Hb was loaded at the following concentrations: 0.2, 1, 5, 15 and 30 μM. The calibration curve was built using conalbumin (75 kDa), ovalbumin (43 kDa) and lysozyme (14 kDa) as standard proteins (Cytiva). The concentrations reported in S2 Fig also consider column dilution, which was approximately 3-fold with respect to the loading concentrations. Data points in S2 Fig were fitted using (Eq. 4):

$$y = a\frac{2[Hb] + K_D - \sqrt{K_D(4[Hb] + K_D)}}{2[Hb]} + y_o$$

where y is the estimated apparent molecular weight, a is the amplitude, corresponding to the apparent molecular weight of the tetramer, [Hb] is the Hb concentration, K_D is the dissociation constant for the Hb dimer/tetramer equilibrium and y_0 is an offset, corresponding to the apparent molecular weight of the Hb dimer.

Acknowledgements

We thank Maisem Laabei, University of Bristol, UK, for kindly providing *Staphylococcus aureus* Newman and the pIMAY* plasmid. We thank Gianmarco Mangiaterra (University of Urbino Carlo Bo, Urbino, Italy) for technical assistance in constructing the pIMAY*Δ*isdB* plasmid. We thank Dr. Davide Cavazzini (Department of Chemistry, Life Sciences and Environmental Sustainability, University of Parma) for technical support in size-exclusion chromatography experiments. This work is dedicated to the memory of Prof. Andrea Mozzarelli, full professor of Biochemistry at the University of Parma who sadly passed away on August 17th, 2024. We are most grateful to Prof. Mozzarelli for his seminal work on

553 hemoglobin allosteric regulation and kinetic mechanisms of sickling that inspired many of us
554 and a plethora of students throughout his scientific and academic career.

555 Author Contribution

556 SB, EF, LR, ODB, MM, FS and FM designed the project and conceptualized the approach;
557 SB, EF, BC, LR, FS, LL and SF supervised the project; SB, FS and EF provided financial
558 resources; EG, SA, BR, FS and LL designed, synthesized and purified C35 compound for
559 assays; SH performed the microbiological assays and analyzed data; FM, MM, VBC and
560 ODB performed the biochemical characterization and analyzed data; CC, VBC and SF
561 performed the ITC measurements and analyzed data; PB performed protein crystallization
562 and structural analysis; SH, FM, MM, VBC, EG, SA, CC and ODB prepared the figures; FM,
563 SB, BC and ODB wrote the original draft; all authors have read and agreed to the published
564 version of the manuscript.

565 Data availability

566 The dataset generated and analyzed in this study has been deposited in the Figshare
567 database under accession code https://doi.org/10.6084/m9.figshare.29145080.
568 Crystallographic model presented in this study is available under accession code 9HBA.

569 References

570 1. Sati H, Carrara E, Savoldi A, Hansen P, Garlasco J, Campagnaro E, et al. The
571 WHO Bacterial Priority Pathogens List 2024: a prioritisation study to guide
572 research, development, and public health strategies against antimicrobial
573 resistance. Lancet Infect Dis. 2025. doi:10.1016/S1473-3099(25)00118-5
574 2. Marchetti M, De Bei O, Bettati S, Campanini B, Kovachka S, Gianquinto E, et al.
575 Iron metabolism at the interface between host and pathogen: From nutritional
576 immunity to antibacterial development. Int J Mol Sci. 2020;21(6):2145.
577 doi:10.3390/ijms21062145
578 3. Mazmanian SK, Skaar EP, Gaspar AH, Humayun M, Gornicki P, Jelenska J, et
579 al. Passage of Heme-Iron Across the Envelope of Staphylococcus aureus.
580 Science. 2003;299:906–9. doi:10.1126/science.1081147

4. De Bei O, Marchetti M, Ronda L, Gianquinto E, Lazzarato L, Chirgadze DY, et al. Cryo-EM structures of staphylococcal IsdB bound to human hemoglobin reveal the process of heme extraction. Proc Natl Acad Sci U S A. 2022;119:e2116708119. doi:10.1073/pnas.2116708119
5. Andrade MA, Ciccarelli FD, Perez-Iratxeta C, Bork P. NEAT: a domain duplicated in genes near the components of a putative Fe3+siderophore transporter from Gram-positive pathogenic bacteria. Genome Biol. 2002;3:research0047.1. doi:10.1186/gb-2002-3-9-research0047
6. Torres VJ, Pishchany G, Humayun M, Schneewind O, Skaar EP. Staphylococcus aureus IsdB is a hemoglobin receptor required for heme iron utilization. J Bacteriol. 2006;188:8421–9. doi:10.1128/JB.01335-06
7. Pietrocola G, Pellegrini A, Alfeo MJ, Marchese L, Foster TJ, Speziale P. The iron-regulated surface determinant B (IsdB) protein from Staphylococcus aureus acts as a receptor for the host protein vitronectin. J Biol Chem. 2020;295:10008–22. doi:10.1074/jbc.RA120.013510
8. Waryah CB, Gogoi-Tiwari J, Wells K, Eto KY, Masoumi E, Costantino P, et al. Diversity of virulence factors associated with west australian methicillin-sensitive staphylococcus aureus isolates of human origin. Biomed Res Int. 2016;2016:8651918. doi:10.1155/2016/8651918
9. Gonzalez JJI, Hossain MF, Neef J, Zwack EE, Tsai C-M, Raafat D, et al. TLR4 sensing of IsdB of Staphylococcus aureus induces a proinflammatory cytokine response via the NLRP3-caspase-1 inflammasome cascade. mBio. 2024;15. doi:10.1128/mbio.00225-23
10. Tsai C-M, Caldera JR, Hajam IA, Chiang AWT, Tsai C-H, Li H, et al. Non-protective immune imprint underlies failure of Staphylococcus aureus IsdB vaccine. Cell Host Microbe. 2022;30:1163-72.e6. doi:10.1016/j.chom.2022.06.006
11. Skaar EP, Schneewind O. Iron-regulated surface determinants (Isd) of Staphylococcus aureus: Stealing iron from heme. Microbes Infect. 2004;6:390–7. doi:10.1016/j.micinf.2003.12.008
12. Cozzi M, Failla M, Gianquinto E, Kovachka S, Buoli Comani V, Compari C, et al. Identification of small molecules affecting the interaction between human

613 hemoglobin and Staphylococcus aureus IsdB hemophore. Sci Rep.
614 2024;14:8272. doi:10.1038/s41598-024-55931-8
615 13. Mozzarelli A, Hofrichter J, Eaton WA. Delay Time of Hemoglobin S
616 Polymerization Prevents Most Cells from Sickling in Vivo. Science.
617 1987;237:500–6. doi:10.1126/science.3603036
618 14. Pishchany G, Haley KP, Skaar EP. Staphylococcus aureus Growth using Human
619 Hemoglobin as an Iron Source. J Vis Exp. 2013. doi:10.3791/50072
620 15. Hammer ND, Skaar EP. Powerful genetic resource for the study of methicillin-
621 resistant Staphylococcus aureus. mBio. 2013. doi:10.1128/mBio.00166-13
622 16. Abdulmalik O, Safo MK, Chen Q, Yang J, Brugnara C, Ohene-Frempong K, et al.
623 5-Hydroxymethyl-2-furfural modifies intracellular sickle haemoglobin and inhibits
624 sickling of red blood cells. Br J Haematol. 2005;128:851-8. doi:10.1111/j.1365-
625 2141.2004.05332.x
626 17. Abdulmalik O, Ghatge MS, Musayev FN, Parikh A, Chen Q, Yang J, et al.
627 Erratum: Crystallographic analysis of human hemoglobin elucidates the structural
628 basis of the potent and dual antisickling activity of pyridyl derivatives of vanillin
629 (Acta Crystallographica Section D (2011) D67 (920-928)). Acta Crystallogr D Biol
630 Crystallogr. 2011;67:929. doi:10.1107/S0907444911045860
631 18. Silva MM, Rogers PH, Arnone A. A third quaternary structure of human
632 hemoglobin A at 1.7-Å resolution. J Biol Chem. 1992;267:17248-56.
633 doi:10.1016/s0021-9258(18)41919-9
634 19. Schumacher MA, Zheleznova EE, Poundstone KS, Kluger R, Jones RT, Brennan
635 RG. Allosteric intermediates indicate R2 is the liganded hemoglobin end state.
636 Proc Natl Acad Sci U S A. 1997;94:7841–6. doi:10.1073/pnas.94.15.7841
637 20. Park SY, Yokoyama T, Shibayama N, Shiro Y, Tame JRH. 1.25 Å Resolution
638 Crystal Structures of Human Haemoglobin in the Oxy, Deoxy and Carbonmonoxy
639 Forms. J Mol Biol. 2006;360:683–96. doi:10.1016/j.jmb.2006.05.036
640 21. Caccia D, Ronda L, Frassi R, Perrella M, Del Favero E, Bruno S, et al.
641 PEGylation promotes hemoglobin tetramer dissociation. Bioconjug Chem.
642 2009;20:1546–55. doi:10.1021/bc900130f
643 22. Liu C, Bo A, Cheng G, Lin X, Dong S. Characterization of the structural and
644 functional changes of hemoglobin in dimethyl sulfoxide by spectroscopic

645 techniques. Biochim Biophys Acta. 1998;1385:181–9. doi:10.1016/S0167-
646 4838(98)00044-2
647 23. Andersen CBF, Stødkilde K, Sæderup KL, Kuhlee A, Raunser S, Graversen JH,
648 et al. Haptoglobin. Antioxid Redox Signal. 2017;26:814–31.
649 doi:10.1089/ars.2016.6793
650 24. Glaros AK, Razvi R, Shah N, Zaidi AU. Voxelotor: alteration of sickle cell disease
651 pathophysiology by a first-in-class polymerization inhibitor. Ther Adv Hematol.
652 2021;12:20406207211001136. doi:10.1177/20406207211001136
653 25. De Bei O, Marchetti M, Guglielmo S, Gianquinto E, Spyrakis F, Campanini B, et
654 al. Time-resolved X-ray solution scattering unveils the events leading to
655 hemoglobin heme capture by staphylococcal IsdB. Nat Commun. 2025;16:1361.
656 doi:10.1038/s41467-024-54949-w
657 26. Kronstad JW, Caza M. Shared and distinct mechanisms of iron acquisition by
658 bacterial and fungal pathogens of humans. Front Cell Infect Microbiol. 2013;3:80.
659 doi:10.3389/fcimb.2013.00080
660 27. Akinbosede D, Chizea R, Hare SA. Pirates of the haemoglobin. Microb Cell.
661 2022;9:60–75. doi:10.15698/MIC2022.04.775
662 28. Abdulmanea AA, Alharbi NS, Somily AM, Khaled JM, Algahtani FH. The
663 Prevalence of the Virulence Genes of Staphylococcus aureus in Sickle Cell
664 Disease Patients at KSUMC, Riyadh, Saudi Arabia. Antibiotics. 2023;12(7):1221.
665 doi:10.3390/antibiotics12071221
666 29. Baba T, Bae T, Schneewind O, Takeuchi F, Hiramatsu K. Genome Sequence of
667 Staphylococcus aureus Strain Newman and Comparative Analysis of
668 Staphylococcal Genomes: Polymorphism and Evolution of Two Major
669 Pathogenicity Islands. J Bacteriol. 2008;190:300–10. doi:10.1128/JB.01000-07
670 30. Schuster CF, Howard SA, Gründling A. Use of the counter selectable marker
671 pheS* for genome engineering in staphylococcus aureus. Microbiology
672 (Reading). 2019;165:1020-30. doi:10.1099/mic.0.000791
673 31. Viappiani C, Abbruzzetti S, Ronda L, Bettati S, Henry ER, Mozzarelli A, et al.
674 Experimental basis for a new allosteric model for multisubunit proteins. Proc Natl
675 Acad Sci U S A. 2014;111:12758–63. doi:10.1073/pnas.1413566111
676 32. Reichlin M. Enzyme Proteins: Hemoglobin and Myoglobin in Their Reactions with
677 Ligands . Eraldo Antonini and Maurizio Brunori. North-Holland, Amsterdam, 1971

(U.S. distributor, Elsevier, New York). xx, 436 pp., illus. $30. Frontiers of Biology, vol. 21. . Science. 1972;178:296. doi:10.1126/science.178.4058.296

33. Gianquinto E, Moscetti I, De Bei O, Campanini B, Marchetti M, Luque FJ, et al. Interaction of human hemoglobin and semi-hemoglobins with the Staphylococcus aureus hemophore IsdB: a kinetic and mechanistic insight. Sci Rep. 2019;9:18944. doi:10.1038/s41598-019-54970-w

34. McCoy AJ, Grosse-Kunstleve RW, Adams PD, Winn MD, Storoni LC, Read RJ. Phaser crystallographic software. J Appl Crystallogr. 2007;40:658–74. doi:10.1107/S0021889807021206

35. Emsley P, Lohkamp B, Scott WG, Cowtan K. Features and development of Coot. Acta Crystallogr D Biol Crystallogr. 2010;66:486–501. doi:10.1107/S0907444910007493

36. Ronda L, Bruno S, Abbruzzetti S, Viappiani C, Bettati S. Ligand reactivity and allosteric regulation of hemoglobin-based oxygen carriers. Biochim Biophys Acta Proteins Proteomics. 2008;1784:1365–77. doi:10.1016/j.bbapap.2008.04.021

37. Hayashi A, Suzuki T, Shin M. An enzymic reduction system for metmyoglobin and methemoglobin, and its application to functional studies of oxygen carriers. Biochim Biophys Acta. 1973;310:306–16. doi:10.1016/0005-2795(73)90110-4

38. Rivetti C, Mozzarelli A, Rossi GL, Henry ER, Eaton WA. Oxygen Binding by Single Crystals of Hemoglobin. Biochemistry. 1993;32:2888–900. doi:10.1021/bi00062a021

Supporting information

S1 Fig. Characterization of the binding of C35 to IsdB. Raw data for ITC titration of 12 μM IsdB with 1 mM C35 (top panel); binding isotherm of the integrated titration curve (bottom panel). The experiment was carried out at 25 °C in 50 mM HEPES buffer, pH 7.6.

S2 Fig. Effect of C35 on the tetramer/dimer equilibrium of oxygenated Hb. (A) Dependence of the apparent molecular weight as a function of Hb concentrations both in the absence (white circles) and presence of 0.01 mM C35 (magenta circles). Data points in the absence of C35 are obtained in the presence of the same DMSO concentration (i.e., 0.1% v/v) with respect to data points obtained in the presence of C35. The fitting of the data (solid lines) to Eq. 3 allowed for the estimation of dissociation constants of about 0.67 ± 0.15

709 and 0.80 ± 0.38 μM for the Hb in the absence and presence of C35, respectively, indicating
710 that the compound does not significantly alter the tetramer-to-dimer equilibrium of Hb. (B)
711 Chromatograms of calibrants (lower panel) used to build the calibration curve (upper panel);
712 CONA, OVA and LISO correspond to conalbumin, ovalbumin and lysozyme, respectively.

713 **S1 Table.** Crystal data and structure refinements for Hb:C35 complex.

714 **S2 Table.** PDB ID, score and corresponding DOI of the first ten structures obtained
715 exploiting "Structure similarity search'' tool on the PDB website
716 (https://www.rcsb.org/search/advanced/structure) and using the structure of Hb bound to
717 C35 as a reference.